Toxicology and Applied Pharmacology 235 (2009) 216–225

Contents lists available at ScienceDirect

Toxicology and Applied Pharmacology

journal homepage: www.elsevier.com/locate/ytaap

Acute and long-term effects after single loading of functionalized multi-walled carbon nanotubes into zebrafish (*Danio rerio*)

Jinping Cheng [a], Chung Man Chan [a], L. Monica Veca [d], Wing Lin Poon [b], Po Kwok Chan [c], Liangwei Qu [d], Ya-Ping Sun [d,*], Shuk Han Cheng [a,*]

[a] Department of Biology and Chemistry, City University of Hong Kong, Hong Kong
[b] Department of Biochemistry (Science), Chinese University of Hong Kong, Hong Kong
[c] Department of Knowledge Transfer Office, City University of Hong Kong, Hong Kong
[d] Department of Chemistry and Laboratory for Emerging Materials and Technology, Clemson University, Clemson, South Carolina 29634-0973, USA

ARTICLE INFO

Article history:
Received 18 September 2008
Revised 18 November 2008
Accepted 4 December 2008
Available online 16 December 2008

Keywords:
Multi-walled carbon nanotubes
Zebrafish
In vivo biodistribution
Long-term effects
Survival
Reproduction potential

ABSTRACT

Carbon nanotubes (CNTs) are widely explored for biomedical applications, but there is very limited information regarding their *in vivo* biodistribution and biocompatibility. Here, we report the *in vivo* biodistribution and long-term effects of functionalized multi-walled carbon nanotubes (MWCNTs) in developing zebrafish. The fluorescent-labeled MWCNTs were introduced into zebrafish embryos at 1-cell stage and at 72 h post fertilization through microinjection. After single injection, both acute and long-term interactions between zebrafish and functionalized MWCNTs were studied. The injected FITC-BSA-MWCNTs (at 1-cell stage) were allocated to all blastoderm cells of the embryos through proliferation, and were distinctively excluded from the yolk cell. When introduced into the circulation system, FITC-BSA-MWCNTs moved easily in the compartments and finally were cleaned out by the body at 96 h after the loading. At early stages, the treated zebrafish embryos generated immune response by accumulating circulating white blood cells at the trunk region. Under transmission electron microscope, many lysosome-like vesicles were observed in the blastoderm cells of the treated embryos. The zebrafish loaded with MWCNTs had normal primordial germ cells at early stage and produced second generation later on. However, the larvae of the second generation had obviously lower survival rates as compared to the untreated groups, suggesting a negative effect on the reproduction potential. These results suggest that extensive purification and functionalization processes can help improve the biocompatibility of CNTs. This study also indicates that purified CNTs may have long-term toxicity effects when they were delivered into the body.

Introduction

Emerging development in nanotechnology shows potential applications such as electronic devices, biological and chemical sensors, and biomaterials. It is expected that half of all drug discovery and delivery technology will be based on nanotechnology by 2015 (Wei, 2005; Emerich and Thanos, 2005). Carbon nanotubes (CNTs) are one of the most widely explored nanomaterials in various fields with their distinctive properties (Klumpp et al., 2006). It is predicted that the global market for CNTs will grow to between $1 billion to $2 billion by 2014 (Thayer, 2007). With the increasing industrial demands and production capacity, a better understanding of how to safely develop and use these engineered nanomaterials is widely concerned.

Previous study showed that contaminants associated with raw CNTs can induce hatching delay in zebrafish embryos (Cheng et al., 2007). Raw CNTs can be purified to remove those associated contaminants, such as metal catalysts (Sun et al., 2002). The purified CNTs can be further chemically modified (Sun et al., 2002), and the chemical modification (functionalization) can help improve the solubility[1] by conjugation with various molecules (Hirsch, 2002; Sun et al., 2002). CNTs have been conjugated with lots of drug molecules (e.g. anticancer, antiviral or antibacterial agents) (Bianco et al., 2005a,b). Previous studies demonstrated that chemically modified CNTs can cross cell membranes and deliver attached cargos

* Corresponding authors. Y.-P. Sun is to be contacted at Department of Chemistry and Laboratory for Emerging Materials and Technology, Clemson University, Clemson, South Carolina 29634-0973, USA. Fax: +864 656 5007. S.H. Cheng, Department of Biology and Chemistry, City University of Hong Kong, Hong Kong. Fax: +852 2788 7406.
E-mail addresses: syaping@clemson.edu (Y.-P. Sun), bhcheng@cityu.edu.hk (S.H. Cheng).

[1] Here the term "solubility" is loosely defined, as it has been commonly used in the literature. One might imagine that the functionalized nanotubes are individually dispersed in the solvent.

0041-008X/$ – see front matter © 2008 Elsevier Inc. All rights reserved.
doi:10.1016/j.taap.2008.12.006

into cells. The *in vivo* biomedical and pharmaceutical explorations of functionalized CNTs have increased dramatically in recent years (Bianco et al., 2005a,b; Klumpp et al., 2006; Liu et al., 2007). The chemically modified CNTs have been studied for targeted delivery with specific biomarkers (Kam and Dai, 2005), diagnostic agents (McDevitt et al., 2007; Wu et al., 2005) as well as therapeutic molecules (Bianco, 2004; Kam et al., 2005; Jia et al., 2003). Modified CNTs have also been investigated as implant materials for medical treatment for bones (Zanello et al., 2006), as well as scaffolds for other tissue engineering purposes (Mattson et al., 2000; Abarrategi et al., 2008).

Before these modified CNTs can be used in the clinic, it is crucial to find out where they go and end up once they are introduced into the body. Furthermore, because of the large number of *in vivo* diagnostics and therapy applications coming from modified CNTs, there may be great potential for the loading of modified CNTs in the biological systems and for the discharge of modified CNTs into the environment. One cannot exclude the possibility that modified CNTs may be found in the organisms once they were released into the environment. However, the information regarding the *in vivo* toxicology study of the modified CNTs in the biological systems is still limited (Nel et al., 2006). One study demonstrated that well dispersed hydroxylated CNTs injected into the mice moved easily in the compartments and tissues and finally accumulated in liver and kidney (Wang et al., 2004) and these modified CNTs have been successfully used for efficient liver tumor targeting (Liu et al., 2007). With the increasing *in vivo* applications of functionalized CNTs, it is important to gain an understanding of their potential *in vivo* biocompatibility and safety in biological systems (Fischer and Chan, 2007). In addition, interactions of these artificial nanomaterials with the human body are very important factors in determining clinical use. Because the nanomaterials incorporated delivery system may be ultimately introduced into the organisms, the information about their *in vivo* biological behavior and consequences becomes very important (Deng et al., 2007). Considering the long-term effect of the *in vivo* applications, chronic impact studies of functionalized nanomaterials such as a full life span analysis are most biologically relevant to determine their biocompatibility and safety (Curtis et al., 2006). To date, however, this kind of information is still very limited.

The purpose of this study was to characterize the *in vivo* biodistribution and long-term effects of functionalized CNTs in developing zebrafish from a whole life span analysis. Fluorescently labeled CNTs modified with functional molecules were used for better and easy tracking in this study. Zebrafish as a small fish species has attracted much interest as remarkable animal models for organogenesis and human disease (Garrity et al., 2002) because they are transparent and grow fast. As well, their organs and tissues are functionally equivalent to those of mammals (Wittbrodt et al., 2002). Using the transparent zebrafish, the *in vivo* biodistribution, biocompatibility and safety of functionalized CNTs in developing zebrafish was investigated. Zebrafish embryos were exposed to BSA-MWCNTs and PPEI-EI-MWCNTs using two different exposure methods including microinjection at 1-cell stage and microinjection into the cardiovascular system at 72 h post fertilization (hpf). This study contributes to *in vivo* biocompatibility and safety study of modified nanomaterials.

Materials and methods

Preparation and characterization of BSA-MWCNTs. Multi-walled CNTs (MWCNTs) were supplied by Nanostructured & Amorphous Materials. The as-supplied MWCNT sample was dispersed in aqueous HNO_3 (2.6 M) and refluxed for 48 h. These purification steps were designed to remove carbonaceous impurities and metal catalysts. The resulting suspension was centrifuged (~1400 *g*), and the sediment was collected and repeatedly washed with deionized water until neutral pH. Upon the removal of water, the sample was dried in vacuum to yield the purified MWCNT sample. The purity of the sample was validated by using thermogravimetric analysis (TGA) on a Mettler Toledo TGA/SDTA851e system with a typical heating rate of 10 °C/min.

The bovine serum albumin (BSA) functionalized MWCNTs (BSA-MWCNTs) were prepared through the amidation reactions (Huang et al., 2002). In a typical experiment, a purified MWCNT sample (35 mg) was homogenized in MES (2-(*N*-morpholino)ethanesulfonic acid) buffer solution (0.1 M, pH=5.6, 20 mL) for 30 min. 1-ethyl-3-(3-dimethylaminopropyl) carbodiimide (EDAC, 200 mg) and *N*-hydroxysuccinimide (NHS, 250 mg) were added to the solution. The mixture was sonicated for 2 h, followed by centrifugation at 6000 rpm for 4 min to keep the sediments. The solid sample was washed with MES buffer solution (0.1 M) 3 times, and then dispersed in PBS buffer solution (pH=7.4, 20 mL) for reaction with BSA (350 mg). After sonication for 2 h and then stirring at room temperature for 48 h, the resulting mixture was transferred to a cellulose ester dialysis membrane tubing (cutoff molecular weight 100,000) for dialysis against fresh water. After 3 days of dialysis, the mixture was centrifuged at 3000 rpm for 10 min to retain the dark-colored supernatant. Upon the evaporation of water, the BSA-MWCNTs sample was obtained. The unused amine groups in BSA (bound to MWCNTs) were targeted for the labeling with the fluorescent dye FITC (fluorescein isothiocyanate). In the experiment, a freshly prepared solution of FITC in DMSO (1 mg/mL) was mixed with an aqueous solution of BSA-MWCNTs (pH=9). The reaction was carried out in the dark at 4 °C for 12 h. The reaction mixture was dialyzed against fresh deionized water for 3 days to obtain the FITC-labeled BSA-MWCNTs sample (FITC-BSA-MWCNTs). The commercially supplied FITC-BSA (Sigma-Aldrich) was used as a control.

Electron microscopy imaging was conducted on a Hitachi HD-2000 scanning transmission electron microscope (S-TEM) operated at 200 kV. Atomic force microscopy (AFM) images were obtained in the acoustic AC mode on a Molecular Imaging PicoPlus system equipped with a multipurpose scanner for a maximum imaging area of 10 μm × 10 μm and a NanoWorld Pointprobe NCH sensor (125 μm in length). The length and height profile analyses were assisted by using the SPIP software distributed by Image Metrology.

The detailed preparation of PPEI-EI-MWCNTs can be found in the supporting information.

Zebrafish maintenance and experimental set-up. Mature zebrafish were purchased from a local commercial source (Chong Hing Aquarium, Hong Kong, China). The zebrafish colony was maintained as described previously (Cheng et al., 2000). Embryos were obtained by photo-induced spawning over green plants and were cultured at 28.5 °C in filtered tap water. The developmental age of the embryos was measured according to the number of hpf and staged according to the method described by Kimmel et al. (1995).

After the light was turned on for photo-induced spawning, embryos were collected within 15 min after fertilization and selected under a dissecting microscope for microinjection at 1-cell stage experiments. Otherwise, embryos were examined at 4 hpf under a dissecting microscope and only embryos that developed normally and reached the blastula stage were selected for cardiovascular loading.

Loading of FITC-BSA-MWCNTs into zebrafish embryos at 1-cell stage by microinjection. The FITC-BSA-MWCNTs were loaded into zebrafish embryos by microinjection at 1-cell stage. Zebrafish embryos were collected into the microinjection plate filled with incubation medium. The FITC-BSA-MWCNTs were then injected into the embryonic cell or yolk of the embryos with a nitrogen-driven micro-injector (Narishige) within 45 min after fertilization. After microinjection, the embryos were incubated at 28.5 °C for further development.

Here is the detailed information for microinjection. Fine-glass microinjection capillary tubes without filament (WPI #TW-100) were pulled and were separated into two microinjection pipettes with Narishige micropipette puller (PC-10). The pipettes were then sharpened with Narishige microforge (MF-900) before use. The microinjection pipette was connected to the micro-injector (Narishige M300 Microinjector) for injection. Microinjection plates were made from 90 mm (diameter)×15 mm (high) Petri dishes. A mold with grooves and bulges was placed to touch the surface of warm molten 1% agarose to produce grooves for trapping eggs for easier injection. The microinjection pipette was calibrated every time before microinjection. About 2 ng of the prepared FITC-BSA-MWCNTs (CNTs equivalent weight) was loaded into the embryo. About 0.54 ng of FITC-BSA (BSA equivalent weight) was loaded into the embryos as a BSA control in some experiments. The dose of FITC-BSA was adjusted according to the BSA amount carried into the cells when the FITC-BSA-MWCNTs were injected.

Biodistribution in the larvae after loading of FITC-BSA-MWCNTs into blood system. The method of microangiography was used to introduce FITC-BSA-MWCNTs into the circulation system of zebrafish embryos. The procedures of microangiography are adopted (Weinstein et al., 1995; Isogai et al., 2003) with some modification. At 4 hpf, embryos were examined under a dissecting microscope and only embryos that developed normally and reached the blastula stage were selected for subsequent experiments. Selected zebrafish embryos at 72 hpf were mounted laterally in 0.3% agarose covered with embryo culture medium. FITC-BSA-MWCNTs were injected into the sinus venous. After injection, FITC-BSA-MWCNTs would circulate throughout the whole vascular network, lighting up each blood vessel with active blood flow from the heart. The embryos loaded with FITC-BSA-MWCNTs in the blood systems were examined after 30 min, 24 h, 48 h and 96 h after microinjection on the Zeiss LSM410 system (LSM 410, Zeiss, Germany) and the confocal images were then further processed for following analysis.

In vivo biodistribution and scoring of phenotypes. The *in vivo* biodistribution of FITC-BSA-MWCNTs loaded at 1-cell stage in developing zebrafish embryos were studied both under a fluorescent and a confocal microscopy. The embryos loaded with FITC-BSA-MWCNTs were scored and imaged under a light microscopy (Nikon Eclipse TE200, Nikon, Japan) at different developmental stages (1–2 cell stage, 50% epiboly, 12 hpf and 24 hpf) before mass pigment formation. To study the intracellular distribution of FITC-BSA-MWCNTs in the embryonic cells, the embryos loaded with FITC-BSA-MWCNTs, and FITC-BSA as a control, were examined under Zeiss LSM410 confocal microscopy (LSM 410, Zeiss, Germany).

Response of embryonic cells after the loading of FITC-BSA-MWCNTs at 1-cell stage. The response of embryonic cells loaded with FITC-BSA-MWCNTs and FITC-BSA were studied under TEM. Zebrafish embryos loaded with FITC-BSA-MWCNTs were collected at 1 hpf and 4 hpf separately. The embryos were fixed in fixation buffer (2% PFA, 2.5% Glutaraldehyde, 0.1 M cacodylate buffer, pH 7.2, 4% sucrose, 1% tannic acid) overnight at 4 °C. The fixed embryos were washed with washing buffer (0.1 M cacodylate buffer (pH 7.2)) for 10 min three times at 4 °C. Then, the embryos were post-fixed with 1% OsO_4 in 0.1 M cacodylate buffer (pH 7.2) at RT for 2 h. The post-fixed embryos were transferred from the washing buffer into the water and then dehydrated gradually with ethanol. The dehydrated embryos were gradually transferred to acetone and then pure resin (Spurr's). The embryos were embedded in pure resin for 4 h at RT, and then the resin was polymerized at 70 °C for 2 days before sectioning. The embryos were sectioned (70 nm) using ultracut UCT (Leica) and placed on copper grids and double stained with 5% uranyl acetate solution and Reynolds' lead citrate solution. The tissue was examined and photographed with a TEM (Philips Tecnai 12 BioTWIN) operating at 80 kV.

Expression pattern of biomarkers in the loaded embryos. Four markers, *MMP9* as the innate immune response marker, *vasa* as a germ line marker, *Zash* as the subset of neurons marker and *MyoD* as the myotomes marker, were analyzed at 24 hpf in embryos loaded with FITC-BSA-MWCNTs using whole mount *in situ* hybridization according to the method described by Westerfield (1995). Antisense RNA for *MMP9*, *vasa, Zash and MyoD* was synthesized by linearizing the plasmids and transcribing with T7 or SP6 polymerase and Digoxigenin-11-UTP (Boehringer, Indianapolis, IN, USA). Zebrafish embryos were loaded with FITC-BSA-MWCNTs at 1-cell stage by microinjection, and were collected and fixed at 24 hpf. Collected embryos were fixed in 4% PFA (Sigma-Aldrich) in PBS at 4 °C overnight, dehydrated in a methanol (MeOH) series and stored in absolute MeOH at −20 °C to increase permeability. Embryos were then digested with Proteinase K (Sigma-Aldrich) and re-fixed before incubation with the antisense probes at 65 °C overnight. Probes were removed with high-stringency washes at 65 °C. Embryos were then incubated with preabsorbed goat serum (Sigma-Aldrich) for 4 h at room temperature. After washing, 5-bromo-4-chloroindolyl phosphate was added as the substrate and nitro blue tetrazolium was added as the coupler (DAKO, Glostrup, Denmark). The FITC-BSA-MWCNTs loaded embryos and untreated control embryos were examined using an inverted microscope (Nikon Eclipse TE200, Nikon, Japan), images of FITC-BSA-MWCNT-treated and untreated control embryos were captured with a cooled color digital camera (TK-C1381, JVC, Japan), and then data was collected and stored using a digital camera attached to a computer.

Staining of cytoskeleton structure and nucleus of the treated embryos. The staining of the microfilament structures and the nucleus of the zebrafish embryos were performed as described in Cheng et al. (2004). For early stage embryos, glass Petri dish was used for removing the chorion and 1% agarose coated Petri dish was used for staining. At sphere epiboly (4 hpf), 50% epiboly, and 75% epiboly, embryos were fixed with 4% PFA in PBS overnight at 4 °C, after which they were washed thoroughly with PBS. All subsequent washing steps were performed for 5 min and were carried out with gentle shaking. To label F-actin and nucleus, embryos were incubated with 0.08 μg/ml Rhodamine–phalloidin (Invitrogen, Carlsbad, CA) and Sytox-green (Invitrogen, Carlsbad, CA), at RT for 1 h in the dark, after which they were washed extensively with PBTD (PBS with 0.1% Tween-20 and 1% DMSO) containing 1% BSA (PBTD/BSA). Images were collected with water immersion Achroplan×20/0.5NA and ×40/0.75NA objectives on the Nikon C1 Confocal Microscopy system (Nikon C1, Nikon, Japan). The FITC and Rhodamine fluorescence was visualized by using 488-nm excitation/520-nm emission and 568-nm excitation/585-nm emission, respectively.

Life cycle effects of FITC-BSA-MWCNTs on the loaded embryos. The survival rates of the zebrafish loaded with FITC-BSA-MWCNTs from 1-cell stage and their offspring were studied. The survival rates of the first generation of zebrafish were recorded at day 14, day 28 and day 56 after the loading of FITC-BSA-MWCNTs and the survival rates of their second generation were recorded at day 14 after birth. The counting was carried out by capturing images by a digital camera without disturbing the zebrafish. Each experiment was conducted on 50 zebrafish embryos loaded with 2 ng of FITC-BSA-MWCNTs at 1-cell stage through injection. All data are presented as the mean±standard deviation (SD) from three separate experiments. Significant differences between mean values were determined using two-way analysis of variance (ANOVA) and Tukey's post hoc test. The two main factors for analysis of variance were treatment and time. The level of statistical significance in all cases was $p<0.05$ at the same studied

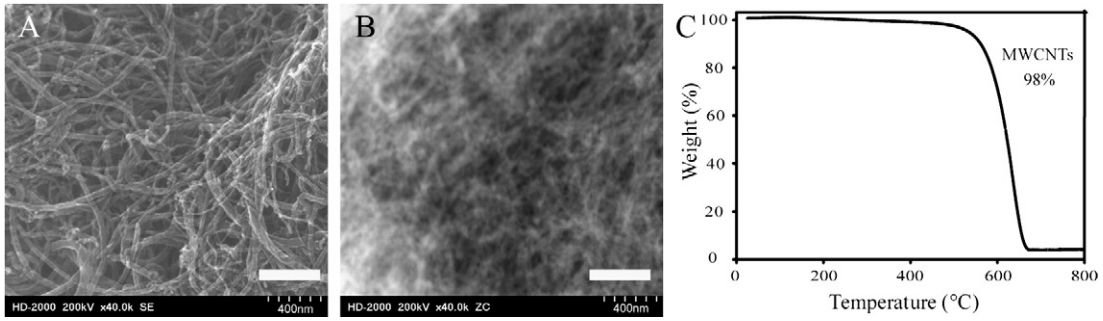

Fig. 1. STEM characterization and TGA analysis of purified MWCNTs. Representative STEM bright-field image (A) showed that purified MWCNTs were quite clear and without obvious amorphous carbon. Corresponding STEM Z-contrast image (B) demonstrated that no metal particles were found by contrast difference in the purified MWCNTs sample. TGA data (C) showed that MWCNTs after purification comprised of 98% of total sample weight. Scale bar: 400 nm.

time point. Percentage data were log-transformed before analysis. The ANOVA was performed using SigmaStat 3.0 software (SPSS, Chicago, IL, USA).

Results

Characterization of prepared BSA-MWCNT sample

MWCNTs, after purification, were studied by TGA and characterized by scanning TEM (S-TEM, Fig. 1) as well as by common SEM and TEM (Supplementary Fig. 1). The S-TEM bright-field image (Fig. 1A) provided the general morphology information on the MWCNTs sample. The Z-contrast mode in S-TEM was used for direct observation of metal particles (residual catalysts from the nanotube production) in the MWCNTs sample because of the large contrast difference between carbon and metals. The Z-contrast image (Fig. 1B) suggested that the purified MWCNTs sample was largely free from metal particles. This was consistent with the TGA result (Fig. 1C).

The carboxylic acid moieties on the surface of purified MWCNTs (derived from the oxidation of surface defect sites) were targeted by BSA (containing amine groups) in the amidation reaction for the covalent conjugation. AFM studies confirmed the successful attachment of BSA to MWCNTs and the well dispersion of BSA-MWCNTs (Fig. 2A). According to statistical analyses of the AFM images (Fig. 2), the average length of BSA-MWCNTs was about 0.8±0.5 μm, and median length 0.7 μm (Fig. 2B), and the average diameter was about 19.9± 8.25 nm, and median diameter 17.5 nm (Fig. 2C).

In vivo biodistribution of FITC-BSA-MWCNTs in developing zebrafish embryos

For the embryos injected with FITC-BSA-MWCNTs (~2 ng per embryo, CNTs equivalent weight) at 1-cell stage, no mortality or developmental defects was observed during all the observed developmental period. At 1–2 cells stage (Fig. 3A), green fluorescence from FITC-BSA-MWCNTs was detected in the blastoderm cells as indicated by the white arrows. The green fluorescent signal associated with FITC-BSA-MWCNTs was then allocated evenly to all of the blastoderm cells through cell division. At 50% epiboly stage, FITC-BSA-MWCNTs signal was concentrated in all blastoderm cells (white arrows in Fig. 3B) and was excluded from the yolk cell. The blastoderm cell preference of FITC-BSA-MWCNTs was also observed in the following

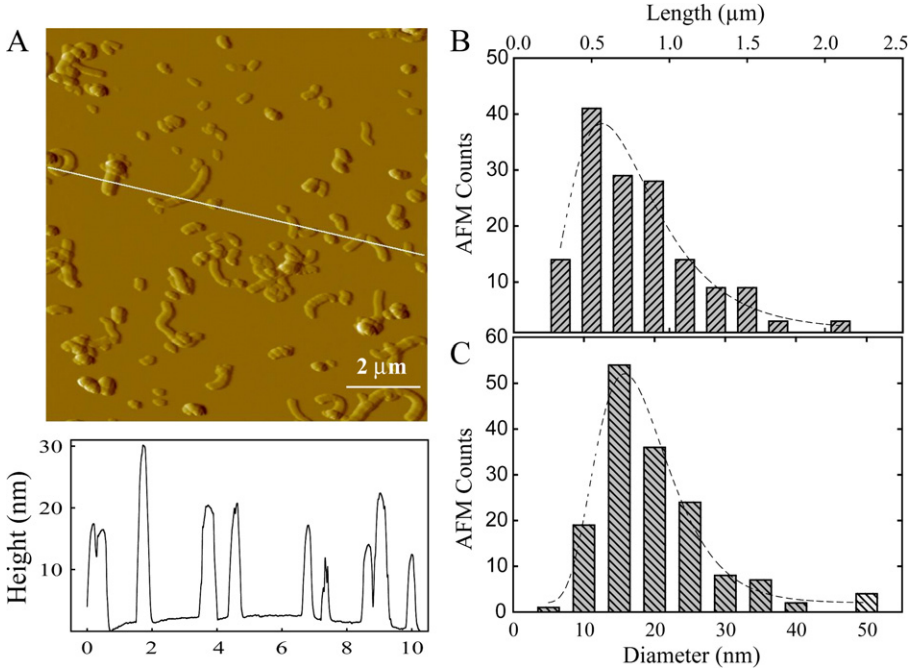

Fig. 2. AFM characterization and size information of BSA-MWCNTs. The BSA-MWCNTs sample was well dispersed and BSA protein was uniformly coated on the surface of MWCNTs as shown by AFM image (A). The length (Mean±SD) of the studied BSA-MWCNTs was 0.8±0.5 μm (B), and the diameter (Mean±SD) of BSA-MWCNTs was 19.9±8.25 nm (C). The scale information is indicated on the AFM image (A).

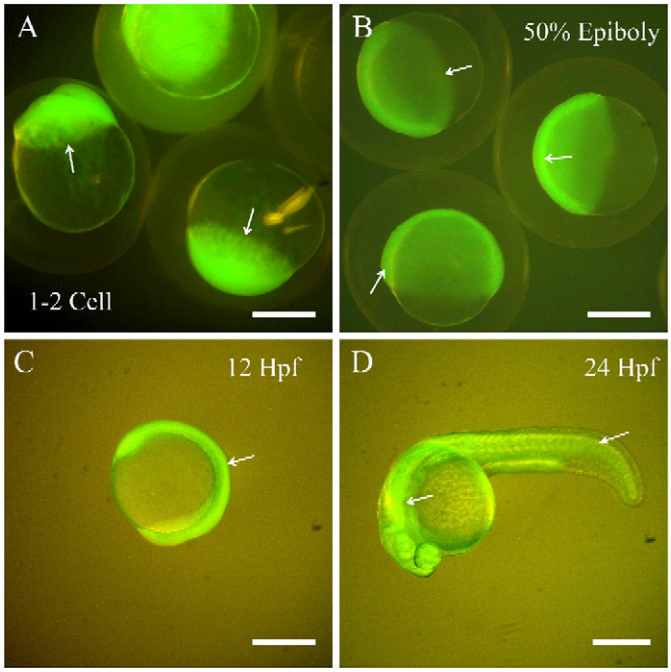

Fig. 3. *In vivo* biodistribution of FITC-BSA-MWCNTs in developing zebrafish embryos at different developmental stages. Zebrafish embryos were loaded with 2 ng of FITC-BSA-MWCNTs (CNTs equivalent weight) at 1-cell stage through microinjection. According to the green fluorescence signal from FITC-BSA-MWCNTs, the loaded FITC-BSA-MWCNTs were distributed in the blastoderm cells but not the yolk cells at all observed developmental stages, including 1–2 cells stage (A), 50% epiboly (B), 12 hpf (C) and 24 hpf (D). Scale bar: 250 μm.

developmental stages, such as at 12 hpf (Fig. 3C) and at 24 hpf (Fig. 3D). When the tissues and organs were already formed, FITC-BSA-MWCNTs could still locate in those blastoderm cells all along the body and kept excluded from the yolk cell (Fig. 3D). The distribution profile of FITC-BSA-MWCNTs was identified again by confocal microscope (Supplementary Fig. 2), and the results demonstrated the same blastoderm cells concentrated distribution.

When FITC-BSA-MWCNTs were injected into the yolk cell of the embryos at 1-cell stage, they showed similar blastoderm cell concentrated distribution although the fluorescent signal was a little bit weaker at first and became intensive later (data not shown). There were frequent exchanges between the blastoderm cells and the yolk cell during early developmental stages of zebrafish embryos. The cytoplasmic stream of the yolk could help FITC-BSA-MWCNTs move to the blastoderm cells although it took longer time for the FITC-BSA-MWCNTs to move to the blastoderm cells in this case as compared to the direct blastoderm cell injection delivery.

Based on the above observations, FITC-BSA-MWCNTs showed higher affinity to the blastoderm cells than the yolk cell. The yolk was known to be composed mainly of lipid to afford energy supply for the embryos at early stages. This result suggested that FITC-BSA-MWCNTs have lower affinity to lipid as compared to the protein enriched intracellular environment.

Intracellular biodistribution of FITC-BSA-MWCNTs in the embryonic blastoderm cells

FITC-BSA-MWCNTs and FITC-BSA were delivered into the embryos at 1-cell stage and both of them accumulated in the blastoderm cells but not in the yolk cell, although there were frequent exchanges between the blastoderm cells and the yolk cell during that period (data not shown, similar as Fig. 3). However, there was a difference in their intracellular distribution (Fig. 4) in the blastoderm cells at 3 hpf. It was noticed that FITC-BSA-MWCNTs remained in both cytoplasm and nucleus of the blastoderm cells (white arrows in Fig. 4A), while FITC-BSA was excluded from the nucleus and stayed only in the cytoplasm of the blastoderm cells (red arrows in Fig. 4B). The cytoplasm and nucleus biodistribution of FITC-BSA-MWCNTs made the green fluorescent signal homogenous in the blastoderm cells (Fig. 4A).

The data suggested that FITC-BSA-MWCNTs can enter the nucleus of blastoderm cells while FITC-BSA cannot. It also suggested that MWCNTs have special property in nuclear membrane penetration. However, there was intensive cell division and the cell proliferation rate was very fast (15 min) at early stage. This nuclear accumulation of FITC-BSA-MWCNTs in blastoderm cells might be a special distribution profile during cell division. Thus, the nuclear accumulation of FITC-BSA-MWCNTs in zebrafish blastoderm cells requires further investigation.

Biodistribution and clearance of FITC-BSA-MWCNTs in zebrafish larvae when loaded into cardiovascular systems

The biodistribution and clearance of FITC-BSA-MWCNTs in zebrafish larvae were studied by introducing FITC-BSA-MWCNTs into the cardiovascular system at 72 hpf through intravascular loading. As shown in Fig. 5, FITC-BSA-MWCNTs first distributed all along the blood circulation system and then moved to the muscles and other tissues easily. It was found that FITC-BSA-MWCNTs went into the floor plate, the brain ventricle, and notochord in the larvae 30 min after the loading (Fig. 5A). The loaded FITC-BSA-MWCNTs finally accumulated

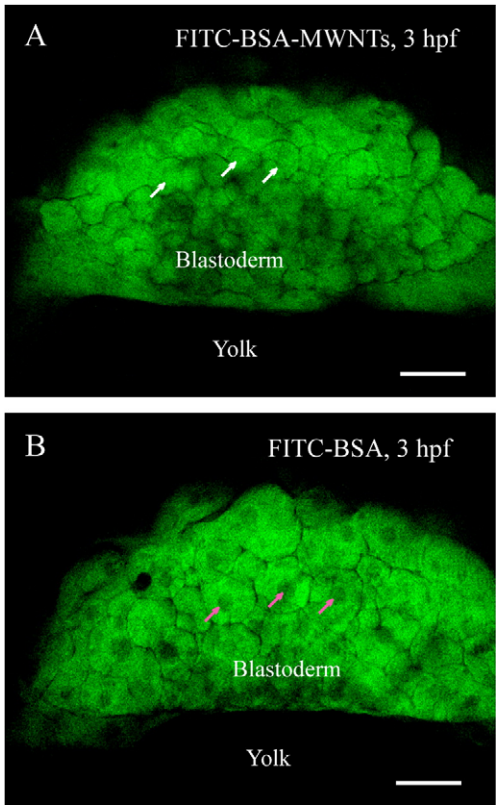

Fig. 4. Representative live images showing intracellular distribution of FITC-BSA-MWCNTs (A) and FITC-BSA (B) in zebrafish embryos at 3 hpf. Both FITC-BSA-MWCNTs and FITC-BSA were delivered into zebrafish embryos at 1-cell stage with 2 ng dosage (CNTs equivalent weight) through microinjection. Both FITC-BSA-MWCNTs and FITC-BSA accumulated in blastoderm cells but not the yolk cells. The loaded FITC-BSA-MWCNTs translocated into the nucleus (white arrows in A) of the blastoderm cells while most FITC-BSA was kept in the cytoplasm of the blastoderm cells (red arrows in B) in the observed time point. Scale bars: 50 μm.

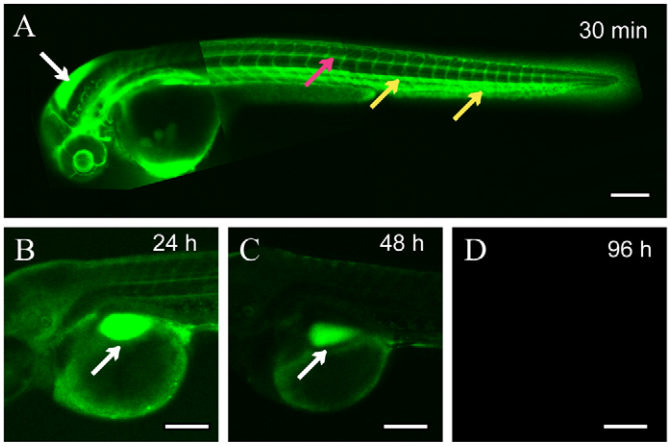

Fig. 5. *In vivo* biodistribution of FITC-BSA-MWCNTs in zebrafish larvae through intravascular loading at 72 hpf. The intravascular loaded FITC-BSA-MWCNTs reached the floor plate (red arrow in A), 4th ventricle (white arrow in A) and blood vessels (yellow arrow in A) within 30 min. Most of the loaded FITC-BSA-MWCNTs gradually accumulated in one swim bladder structured region of the larvae at 24 h (white arrow in B) and 48 h (white arrow in C) after the delivery. The intravascular loaded FITC-BSA-MWCNTs were gradually excreted out from the embryos, and there was no detectable signal at around 96 h after the delivery (D). Scale bar: 200 μm.

at one specific region, a swim bladder structured organ, after 24 h (Fig. 5B) and 48 h (Fig. 5C) of delivery. Examination of frozen sections confirmed that the FITC-BSA-MWCNTs were adsorbed by the tissues and accumulated in different organs (Supplementary Fig. 3). The injected FITC-BSA-MWCNTs had a relatively long circulation time as compared to normal dyes or other nanomaterials, which took less than 24 h (Cheng et al., 2001).

Zebrafish larvae exhibited highly concentrated FITC-BSA-MWCNTs in the swim-bladder structured organ, but no detectable fluorescent signal of FITC-BSA-MWCNTs was observed from other organs after 48 h. Fluorescent intensity from FITC-BSA-MWCNTs in the swim-bladder structured organ was concentrated from other tissues, which suggested that the swim bladder structured organ has a priority to accumulate FITC-BSA-MWCNTs particles. Since the swim bladder is known as a detoxifying organ, the results indicated that the zebrafish larvae managed to clean out the injected carbon nanoparticles effectively. These FITC-BSA-MWCNTs were gradually excreted out from zebrafish larvae, and there was no detectable signal at around 96 h after delivery (Fig. 5D).

Cellular response of embryonic cells after loaded with FITC-BSA-MWCNTs

The cellular response of the embryonic cells of zebrafish embryos after the loading of FITC-BSA-MWCNTs was investigated under TEM. The embryos were fixed and ultra-sectioned and then the samples were investigated under the TEM to observe the cellular response. Many lysosome-like vesicles came up within 15 min after FITC-BSA (Fig. 6B) and FITC-BSA-MWCNTs (Fig. 6C) were delivered into the embryos at 1-cell stage (white arrows in Figs. 6B and C), while untreated control embryos did not have such vesicles (Fig. 6A). These vacuole structures still existed at 4 hpf, more than 3 h after the loading

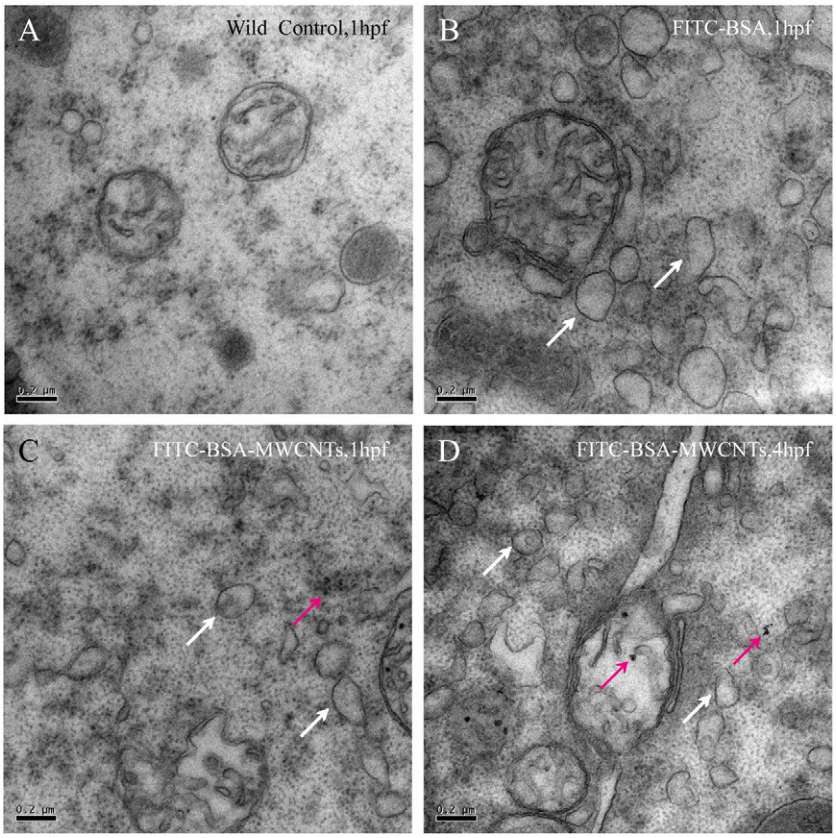

Fig. 6. Cellular responses of the embryonic blastoderm cells to the loading of MWCNTs. Many lysosome-like vesicles formed within 15 min after FITC-BSA (B) and FITC-BSA-MWCNTs (C) were delivered into the embryos at 1-cell stage (see white arrows in B and C), while untreated control embryos did not have such vesicles (A). These lysosome-like vesicles existed at 4 hpf which is more than 3 h after the loading of FITC-BSA-MWCNTs (D). The loaded FITC-BSA-MWCNTs were randomly distributed in the blastoderm cells (see red arrows in C and D). Scale bar: 200 nm.

of FITC-BSA-MWCNTs. The continuous presence of vacuole structures suggested that the blastoderm cells were trying to remove those carbon nanoparticles after the invasive loading. The blastoderm cells had similar cellular response to FITC-BSA-MWCNTs as compared to FITC-BSA (Figs. 6B and C), indicating that the forming of the lysosome-like vesicles is a general phenomenon. These vesicles may be lysosomes since lysosomes are digestive organelles. One study on the translocation of fullerenic nanoparticles has also found that many lysosome-like vesicles were formed after the fullerenic nanoparticles were internalized by the mammalian cells (Li et al., 2008).

It was noticed that FITC-BSA-MWCNTs, present as small aggregates, were randomly located in the blastoderm cells without specific preference to the intracellular organelles (red arrows in Figs. 6C and D).

Immune response after the delivery and the primordial germ cells

The phenotype scoring analysis showed no obvious deformation or malformation in the treated zebrafish embryos to adult stages as compared to the wild type controls. The morphological images of the treated embryos at 4 hpf and 6 hpf showed that the injected embryos developed normally (Supplementary Fig. 4).

The immune responses of the embryos loaded with MWCNTs were studied using *MMP9* as the marker. Members of the Matrix Metalloproteinases (*MMPs*) family are important for the remodeling of the extracellular matrix in a number of biological processes including a variety of immune responses (Yoong et al., 2007). One member of the family, *MMP9*, also known as gelatinase B, is highly expressed in specific myeloid cell populations in which they play a role in the innate immune response (Yoong et al., 2007).

To determine the spatial expression pattern of *MMP9* with and without the loading of MWCNTs, whole mount *in situ* hybridization was performed and the results are shown in Fig. 7. The embryos, loaded with 2 ng of MWCNTs at 1-cell stage, showed a change in *MMP9* expression level and pattern (red arrowhead in Fig. 7B), as compared to the control embryos (dark arrowhead in Fig. 7A). It is known that *MMP9* expression from 24 hpf was presented in a population of circulating white blood cells, which migrates to the site of trauma (Yoong et al., 2007). The circulating white blood cells marked by *MMP9* expression (visualized by the blue color) were localized in the head region near the eye (data not shown), and along the trunk of the embryos at 24 hpf (Fig. 7A). When the embryos were loaded with MWCNTs, the signal for *MMP9* increased noticeably in the trunk region, while the distribution of the circulating blood cells was concentrated in certain regions (Fig. 7B). The *MMP9* was previously found to be significantly up-regulated in the zebrafish larvae in response to exposure of low levels of cadmium chloride and methyl mercury chloride (Yang et al., 2007). Our results suggested that zebrafish embryos may generate innate immune response at later developmental stages when being injected with MWCNTs at 1-cell stage.

The effects on the reproduction system by loading MWCNTs into embryos at 1-cell stage were evaluated using *vasa* as a germ line marker since early life stages are generally most sensitive to toxic effects. The gene expression profiles of *vasa* in embryos loaded with MWCNTs and untreated control embryos were studied. The primordial germ cells marked by *vasa* (red arrow in Fig. 7D) in the treated embryos were not affected as compared to the control (dark arrow in Fig. 7C). The results indicated that embryos loaded with MWCNTs from 1-cell stage maintained a proper reproductive systems and the production of germ cells was not affected.

Using the myogenic regulatory factor, *MyoD*, as a marker, the myotomes were found to be well organized, with arrowhead-shaped alignment both in MWCNT-exposed and control embryos (Supplementary Figs. 5A & B). The subset of neurons in the peripheral cuticular and central nervous systems in the treated zebrafish embryos were well developed (Supplementary Figs. 5C & D) as determined using zebrafish achaete-scute homolog (*zash*), as the marker. All of the molecular and cellular experimental results provided further evidence that the exposed embryos developed normally.

Influence on cytoskeleton structure and nucleus distribution

The cytoskeleton staining results showed that the microfilament structure of the treated embryos was quite intact and was not disturbed by the loaded MWCNTs as compared with the control (Supplementary Fig. 6). After mass cell proliferation, the embryos loaded with MWCNTs proceeded cell migration successfully and formed the nucleus of yolk syncytial layer at 4 hpf and 5.3 hpf (white dots marked area in Figs. 8D and E), which is similar as the control (white dots marked area in Figs. 8A and B). As the F-actin marks the cell boundary, the cell morphology and size information could be derived from F-actin staining. The F-actin staining combined with nucleus staining results revealed that the embryos loaded with MWCNTs had associated and well organized cells (Fig. 8D and E) as untreated control embryos (Figs. 8A and B). The nucleus of the enveloping and deep layer cells of the treated embryos were well organized as the untreated control (yellow arrowhead in Fig. 8). No apoptosis was observed in the studied embryos. The treated embryos had the continuous punctuate band of actin at the leading edge of the enveloping layer (yellow arrow in Fig. 8C) at 75% epiboly as the control (yellow arrow in Fig. 8F).

The cytoskeleton structure is important for maintaining cell morphology and complex function of the cell components. When MWCNTs went into the blastoderm cells of the embryos, the cells had to distinguish MWCNTs from their own cytoskeleton structure because MWCNTs shared similar fibers structure and size as that of the microfilaments and microtubules in the blastoderm cells. As the embryos loaded with MWCNTs proceeded to normal development for more than 3 days, the embryos seemed to have their own way to recognize the microfilament structures from MWCNTs.

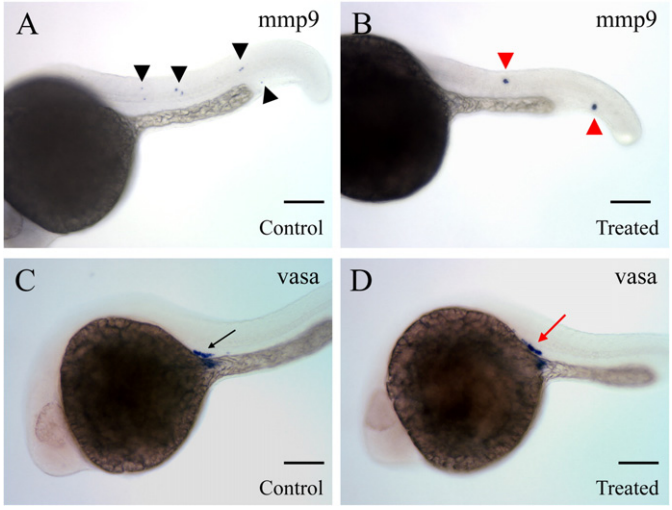

Fig. 7. Whole mount *in situ* hybridization with *MMP9* (A, B) and *Vasa* (C, D) labeled probes at 24 hpf on wild type and MWCNTs loaded embryos. The circulating white blood cells showed expression of *MMP9* (blue color) along the trunk. The expression profile of *MMP9* in the embryos loaded with FITC-BSA-MWCNTs (B) was changed and up-regulated through accumulation of white blood cells (red arrowheads in B) as compared to the control (dark arrowheads in A). The gene expression pattern of *vasa* was not obviously affected in the embryos loaded with FITC-BSA-MWCNTs (red arrow in D) compared to the control (dark arrow in C). The arrowheads and arrows indicate the position of cells expressing *MMP9* and *Vasa* respectively. Scale bar: 150 μm.

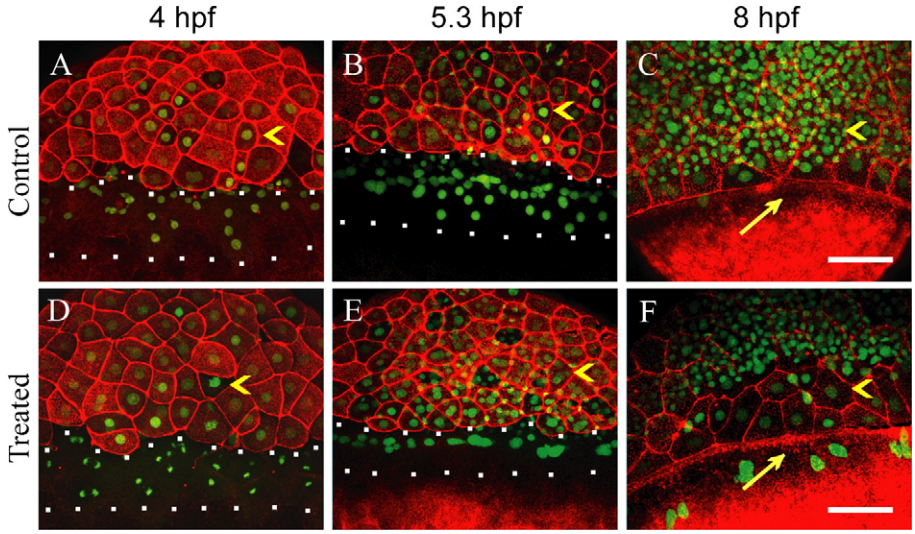

Fig. 8. Effects of BSA-MWCNTs on the cytoskeleton structure of the treated embryos. Representative F-actin and nucleus staining images of embryos loaded with 2 ng (CNTs equivalent weight) of FITC-BSA-MWCNTs (D, E, F) and wild type control (A–C) at 4, 5.3 and 8 hpf (n=8). Red signal indicated the F-actin by Rhodamine-phalloidin staining and green signal is the Sytox-green staining results of the nucleus. White dots surrounded area indicates the yolk syncytial layer. Yellow arrowheads point to specific cells with one nucleus inside the cell boundary marked by F-actin. Yellow arrows point to the continuous punctuate band of actin at the leading edge of the enveloping layer. Each image is a projected stack of confocal optical sections. Scale bar: 50 μm.

Life cycle effects on the survival rates and the reproduction of next generation

A life-cycle test with zebrafish was carried out with the loading of FITC-BSA-MWCNTs as well as PPEI-EI-MWCNTs at 1-cell stage under normal fish culture conditions. The survival rates of the first generation of the zebrafish loaded with FITC-BSA-MWCNTs and PPEI-EI-MWCNTs at different developmental stages were compared with the wild type control. Similar survival rates were observed in both treated and untreated groups, as shown in Fig. 9A and Supplementary Fig. 7A respectively. Larval development was not delayed, and after reaching maturity, these MWCNT-treated fishes performed spawning and produced next generation normally. Effects on spawning were not influenced by the loading of MWCNTs, which was coincided with the above primordial germ cell expression study.

A significant reduction of survival rates of the second generation, as illustrated in Fig. 9B and Supplementary Fig. 7B respectively, was found in the fish loaded with FITC-BSA-MWCNTs and PPEI-EI-MWCNTs at day 14. The embryos loaded with MWCNTs from the beginning of development possessed normal survival rates and produced next generation properly but the second generation showed decreased survival rates. Although the underlying mechanism is unknown, these findings indicate that the further reproduction potential of fish populations might be disturbed by a long-term loading with MWCNTs from fertilization until sexual maturity.

Discussion

Safe manufacturing and application of nanomaterials is an emerging issue with the bloom of nanotechnology (Medina et al., 2007). Understanding the interaction of CNTs with the biological system is essential for the realization of their safe applications. Well functionalized MWCNTs were used to investigate the *in vivo* distribution of modified carbon nanoparticles in zebrafish. The findings gathered in this study help to determine the interaction, behavior and potential toxicity of coated nanomaterials in the developing biological organisms. When MWCNTs were delivered into zebrafish through microinjection into the cells, they mainly concentrated in the blastoderm cells but not in the yolk cell. Previous study reported that fluorescent polystyrene nanoparticles accumulated in the oil droplets of medaka embryos (Kashiwada, 2006) by direct exposure. In this study, fluorescent dye FITC labeled MWCNTs were excluded from the yolk cell in zebrafish embryos. A study of the

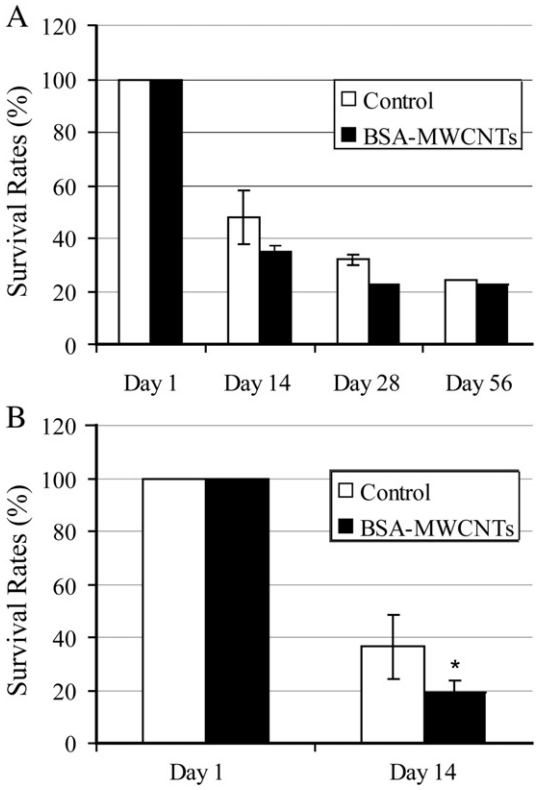

Fig. 9. Survival rates (mean±SD) of zebrafish *(Danio rerio)* loaded with BSA-MWCNTs (A) and larval survival rates (mean±SD) of their second generations (B). The survival rates of zebrafish loaded with BSA-MWCNTs from 1-cell stage and control at day 14, day 28 and day 56 were shown in dark and blank, respectively. The zebrafish loaded with BSA-MWCNTs had similar survival rates as compared to the control at all studied developmental stages (A). The offspring of the zebrafish loaded with BSA-MWCNTs at 1-cell stage had significant lower survival rates as compared to that of control (B) (p<0.05). The survival rates indicate the survival percentage of each case (n=50) from three experiments (n=150).

distribution of water-miscible C_{60} fullerene in rats (Yamago et al., 1995) found that 91.7% of intravenously administered water-miscible fullerene was distributed to the liver. However, in this study, the intravascular loaded MWCNTs mainly accumulated in the swim bladder structured organ but not in the liver. This distribution difference may be caused by the specific nanoparticles. The exposure route may also play a role in the bioaccumulation process considering the different administrative methods used. Multiple physicochemical and environmental factors should also be considered (Hardman, 2006). The distribution profile difference suggests that nanoparticles may generate different biological effects in the biological systems, and one kind of nanoparticles may also show different impacts if administrated differently.

This study investigated the biocompatibility of MWCNTs in an aquatic organism, zebrafish, through both acute and whole life span analysis. There was no lethal effect upon exposure and no developmental defects were observed in the treated zebrafish. The embryos loaded with MWCNTs from 1-cell stage preceded to cell proliferation properly and survived well in the whole life span. It might be the strong maternal control effect at the early development stage, which guaranteed correct cell proliferation even with minor interruptions, such as loading with the invaded MWCNTs. Another study also reported that well purified and functionalized CNTs did not exert genetic toxicity in mammalian cells in terms of cell cycle distribution and cell division upon 5 days continuous exposure (Cheng et al., 2008).

When it comes to the cell migration movements, which are dependent on the zygotic control, the embryos initiated the epiboly with its own zygotic controlled genetic information. It was noticed that the cell movement was not disturbed by the loaded fiber structured CNTs. The MWCNT-treated embryos exerted immune response and the circulating white blood cells relocated in the body, and those interrupted blastoderm cells tried to produce many vesicles to remove the invaded foreigners. These responses suggest that the treated embryos are trying to clean up the loaded MWCNTs. After being loaded into the circulation system, the MWCNTs penetrated the blood-brain barrier and reached the brain ventricle, gradually accumulated into swim bladder region and finally were cleaned up by the body. There is a cleaning up mechanism in response to the intravascular loading in zebrafish larvae. The removal comparison between these two administration methods suggests that the intravascular loading is more useful when considering MWCNTs as the drug carrier since the intravascular loading strategy can remove the nanomaterials after their delivery functions in the body.

Early life stages are generally most sensitive to toxicant exposure. The 1-cell stage injection should be more sensitive as compared to circulation system injection at 72 h post fertilization. For example, zebrafish embryos get tolerant to some treatments post 3 days of embryonic development, such as morpholino. Considering that the 1-cell stage injection is more sensitive to toxicant exposure while circulation system injection might be more potentially used in clinic purposes, both 1-cell stage injection and circulation system injection were used. However, most of the toxicology study end points in this study were taken from 1-cell stage injection.

The development and reproduction of fish are highly complex processes and a number of studies have demonstrated that these processes, including growth, sexual differentiation, and maturation of gametes and spawning, can be adversely affected by metals and organic pollutants at sublethal concentrations (Van den et al., 2003). Development and reproduction is an important issue when considering the long term effect of releasing nanomaterials into the environment or incorporating the nanomaterials into the organisms. Several molecular markers for primordial germ cells have been identified for zebrafish. One of these is *vasa*, which is expressed at all developmental stages of the developing germ line, except mature sperm (Raz, 2003). The transcripts of *vasa* serve as a marker for the developing germ line in the zebrafish (Yoon et al., 1997; Krovel and Olsen, 2002). Toxicant exposures may affect critical events in the development of the reproductive system, ranging from early primordial germ cells determination to gonad differentiation, gametogenesis, external genitalia, or signaling events regulating sexual behavior (Pryor et al., 2000). The zebrafish loaded with MWCNTs formed primordial germ cells at early stage and produced second generation. However, their offspring had significant lower survival rates at larvae stage as compared to the untreated groups. The results showed a negative impact on the reproduction potential in the long term for the loaded zebrafish.

It has been reported that survival rates of zebrafish (Danio rerio) are different in different origins (Diekmann and Nagel, 2005). The survival rates of zebrafish from one species can also vary much depending on the diet and method of food delivery. Survival rates were reported in the range of ~15–80% through 28 days post fertilization (Goolish et al., 1999). In this study, all of the control and treated zebrafish were raised up with the same diet and food delivery method. The survival rates comparison between the control and treatment groups can help determine the effect of loading with MWCNTs on the zebrafish survival along their life span. In this study we did not observe obvious difference in terms of biodistribution and survival rates among two surface molecules, PPEI-EI and BSA. The similar *in vivo* biodistribution pattern and survival rates after the exposure to MWCNTs modified with different surface molecules may suggest that MWCNTs played an important role in the *in vivo* biodistribution pattern in zebrafish.

The biocompatibility of nanomaterials is an important factor for their potential *in vivo* applications. Experimental data showed modification of nanoparticles can also change their *in vitro* behavior (Nimmagadda et al., 2006). These modifications may result in unanticipated effects both on the material's properties as well as the organisms exposed to the nanomaterial. Another related study also illustrated that the cytotoxic response of cells in culture is dependant on the degree of functionalization of the CNTs (Sayes et al., 2006). Raw MWCNTs has been found to induce inflammatory and fibrotic responses in the lungs of treated rats (Muller et al., 2005). The present study showed that well purified and modified MWCNTs did not exert serious toxic impacts in the loaded zebrafish, at least in their own life span. This study suggests that intensive purification and functionalization processes can help improve the biocompatibility of CNTs in the biological systems. The studied MWCNTs were composed of 98% of the sample. The remaining 2% residues effect was minimized by the further functionalization process. The chemical modification process added BSA protein on the surface of MWCNTs and this surface modification can help decrease their potential toxicity and increase their biocompatibility when loaded into the biological systems.

With the typically small amount of modified nanoparticles being produced in each batch, it is essential to gather knowledge about how each step of chemical production and modification would generate harmful side products. This present study explored the application of zebrafish as a test system for *in vivo* nanotoxicology. The zebrafish system only takes up a small amount of test nanomaterials and provides easy tracking on biodistribution and subsequent biological responses within the transparent embryos. Zebrafish embryos offer an inexpensive and ethically acceptable vertebrate model that will not only be useful in the toxicological assessment of the tens of thousands of compounds to be tested, but can also help to evaluate the developmental toxicity of novel compounds at an early stage of drug development. The zebrafish test system can be further applied for the *in vivo* evaluation of the emerging nanomaterials as well as other emerging compounds.

Conflict of interest statement

The authors declare that there are no conflicts of interest.

Acknowledgments

The work described in this paper was substantially supported by a grant from the Research Grants Council of the Hong Kong SAR (Project No. CityU 160108) to S. H. Cheng. The Clemson group was supported by the U.S. National Science Foundation. K. A. S. Fernando and F.S. Lu are thanked for experimental assistance. C. N. Cheng is thanked for the help of microfilament staining. C. W. Cheng is thanked for the help of cryo-section. The MMP9 plasmid is a kind gift from Prof. U. Strähle′ s lab at Institute of Toxicology and Genetics in Forschungszentrum Karlsruhe, Germany. Michelle Hui is thanked for her critical reading of our paper.

Appendix A. Supplementary data

Supplementary data associated with this article can be found, in the online version, at doi:10.1016/j.taap.2008.12.006.

References

Abarrategi, A., Gutierrez, M.C., Moreno-Vicente, C., Hortiguela, M.J., Ramos, V., Lopez-Lacomba, J.L., Ferrer, M.L., del, M.F., 2008. Multiwall carbon nanotube scaffolds for tissue engineering purposes. Biomaterials 29, 94–102.

Bianco, A., 2004. Carbon nanotubes for the delivery of therapeutic molecules. Expert Opin. Drug Deliv. 1, 57–65.

Bianco, A., Kostarelos, K., Partidos, C.D., Prato, M., 2005a. Biomedical applications of functionalised carbon nanotubes. Chem. Commun. (Cambridge, U. K.) 5, 571–577.

Bianco, A., Kostarelos, K., Prato, M., 2005b. Applications of carbon nanotubes in drug delivery. Curr. Opin. Chem. Biol. 9, 674–679.

Cheng, S.H., Wai, A.W.K., So, C.H., Wu, R.S.S., 2000. Cellular and molecular basis of cadmium-induced deformities in zebrafish embryos. Environ. Toxicol. Chem. 19, 3024–3031.

Cheng, S.H., Chan, P.K., Wu, R.S., 2001. The use of microangiography in detecting aberrant vasculature in zebrafish embryos exposed to cadmium. Aquat. Toxicol. 52, 61–71.

Cheng, J.C., Miller, A.L., Webb, S.E., 2004. Organization and function of microfilaments during late epiboly in zebrafish embryos. Dev. Dyn. 231, 313–323.

Cheng, J., Flahaut, E., Cheng, S.H., 2007. Effect of carbon nanotubes on developing zebrafish (*Danio rerio*) embryos. Environ. Toxicol. Chem. 26, 708–716.

Cheng, J., Fernando, K.A.S., Veca, L.M., Sun, Y.P., Lamond, A.I., Lam, Y.W., Cheng, S.H., 2008. Reversible accumulation of PEGylated single-walled carbon nanotubes in the mammalian nucleus. ACS Nano 2 (10), 2085–2094.

Curtis, J., Greenberg, M., Kester, J., Phillips, S., Krieger, G., 2006. Nanotechnology and nanotoxicology: a primer for clinicians. Toxicol. Rev. 25, 245–260.

Deng, X., Jia, G., Wang, H., Sun, H., Wang, X., Yang, S., Wang, T., Liu, Y., 2007. Translocation and fate of multi-walled carbon nanotubes in vivo. Carbon 45, 1419–1424.

Diekmann, M., Nagel, R., 2005. Different survival rates in zebrafish (*Danio rerio*) from different origins. J. Appl. Ichthyol. 21 (5), 451–454.

Emerich, D.F., Thanos, C.G., 2005. Nanomedicine. Curr. Nanosci. 1, 177–188.

Fischer, H.C., Chan, W.C., 2007. Nanotoxicity: the growing need for in vivo study. Curr. Opin. Biotechnol. 18, 565–571.

Garrity, D.M., Childs, S., Fishman, M.C., 2002. The heartstrings mutation in zebrafish causes heart/fin Tbx5 deficiency syndrome. Development 129, 4635–4645.

Goolish, E.M., Okutake, K., Lesure, S., 1999. Growth and Survivorship of larval zebrafish *Danio rerio* on processed diets. N. Am. J. Aquac. 61, 189–198.

Hardman, R., 2006. A toxicologic review of quantum dots: toxicity depends on physicochemical and environmental factors. Environ. Health Perspect. 114, 165–172.

Hirsch, A., 2002. Functionalization of single-walled carbon nanotubes. Angew. Chem. Int. Ed. Engl. 41, 1853–1859.

Huang, W.J., Taylor, S., Fu, K.F., Lin, Y., Zhang, D.H., Hanks, T.W., Rao, A.M., Sun, Y.P., 2002. Attaching proteins to carbon nanotubes via diimide-activated amidation. Nano Lett. 2, 311–314.

Isogai, S., Lawson, N.D., Torrealday, S., Horiguchi, M., Weinstein, B.M., 2003. Angiogenic network formation in the developing vertebrate trunk. Development 130, 5281–5290.

Jia, L., Wong, H., Wang, Y., Garza, M., Weitman, S.D., 2003. Carbendazim: disposition, cellular permeability, metabolite identification, and pharmacokinetic comparison with its nanoparticle. J. Pharm. Sci. 92, 161–172.

Kam, N.W., Dai, H., 2005. Carbon nanotubes as intracellular protein transporters: generality and biological functionality. J. Am. Chem. Soc. 127, 6021–6026.

Kam, N.W., Liu, Z., Dai, H., 2005. Functionalization of carbon nanotubes via cleavable disulfide bonds for efficient intracellular delivery of siRNA and potent gene silencing. J. Am. Chem. Soc. 127, 12492–12493.

Kashiwada, S., 2006. Distribution of nanoparticles in the see-through medaka (*Oryzias latipes*). Environ. Health Perspect. 114, 1697–1702.

Kimmel, C.B., Ballard, W.W., Kimmel, S.R., Ullmann, B., Schilling, T.F., 1995. Stages of embryonic-development of the zebrafish. Dev. Dyn. 203, 253–310.

Klumpp, C., Kostarelos, K., Prato, M., Bianco, A., 2006. Functionalized carbon nanotubes as emerging nanovectors for the delivery of therapeutics. Biochim. Biophys. Acta 1758, 404–412.

Krovel, A.V., Olsen, L.C., 2002. Expression of a vas::EGFP transgene in primordial germ cells of the zebrafish. Mech. Dev. 116, 141–150.

Li, W., Chen, C., Ye, C., Wei, T., Zhao, Y., Lao, F., Chen, Z., Meng, H., Gao, Y., Yuan, H., Xing, G., Zhao, F., Chai, Z., Zhang, X., Yang, F., Han, D., Tang, X., Zhang, Y., 2008. The translocation of fullerenic nanoparticles into lysosome via the pathway of clathrin-mediated endocytosis. Nanotechnology 19, 145102.

Liu, Z., Cai, W., He, L., Nakayama, N., Chen, K., Sun, X., Chen, X., Dai, H., 2007. In vivo biodistribution and highly efficient tumour targeting of carbon nanotubes in mice. Nat. Nano 2, 47–52.

Mattson, M.P., Haddon, R.C., Rao, A.M., 2000. Molecular functionalization of carbon nanotubes and use as substrates for neuronal growth. J. Mol. Neurosci. 14, 175–182.

McDevitt, M.R., Chattopadhyay, D., Kappel, B.J., Jaggi, J.S., Schiffman, S.R., Antczak, C., Njardarson, J.T., Brentjens, R., Scheinberg, D.A., 2007. Tumor targeting with antibody-functionalized, radiolabeled carbon nanotubes. J. Nucl. Med. 48, 1180–1189.

Medina, C., Santos-Martinez, M.J., Radomski, A., Corrigan, O.I., Radomski, M.W., 2007. Nanoparticles: pharmacological and toxicological significance. Br. J. Pharmacol. 150, 552–558.

Muller, J., Huaux, F., Moreau, N., Misson, P., Heilier, J.F., Delos, M., Arras, M., Fonseca, A., Nagy, J.B., Lison, D., 2005. Respiratory toxicity of multi-wall carbon nanotubes. Toxicol. Appl. Pharmacol. 207, 221–231.

Nel, A., Xia, T., Madler, L., Li, N., 2006. Toxic potential of materials at the nanolevel. Science 311, 622–627.

Nimmagadda, A., Thurston, K., Nollert, M.U., McFetridge, P.S., 2006. Chemical modification of SWNT alters in vitro cell-SWNT interactions. J. Biomed. Mater. Res. A. 76, 614–625.

Pryor, J.L., Hughes, C., Foster, W., Hales, B.F., Robaire, B., 2000. Critical windows of exposure for children's health: the reproductive system in animals and humans. Environ. Health Perspect. 108 Suppl 3, 491–503.

Raz, E., 2003. Primordial germ-cell development: the zebrafish perspective. Nat. Rev. Genet. 4, 690–700.

Sayes, C.M., Liang, F., Hudson, J.L., Mendez, J., Guo, W., Beach, J.M., Moore, V.C., Doyle, C.D., West, J.L., Billups, W.E., Ausman, K.D., Colvin, V.L., 2006. Functionalization density dependence of single-walled carbon nanotubes cytotoxicity in vitro. Toxicol. Lett. 161, 135–142.

Sun, Y.P., Fu, K.F., Lin, Y., Huang, W.J., 2002. Functionalized carbon nanotubes: properties and applications. Acc. Chem. Res. 35, 1096–1104.

Thayer, A.M., 2007. Carbon nanotubes by the metric ton. Chem. Eng. News 85, 29–35.

Van den, B.K., Verheyen, R., Witters, H., 2003. Effects of 17alpha-ethynylestradiol in a partial life-cycle test with zebrafish (*Danio rerio*): effects on growth, gonads and female reproductive success. Sci. Total Environ. 309, 127–137.

Wang, H., Wang, J., Deng, X., Sun, H., Shi, Z., Gu, Z., Liu, Y., Zhao, Y., 2004. Biodistribution of carbon single-wall carbon nanotubes in mice. J. Nanosci. Nanotechnol. 4, 1019–1024.

Wei, C.M., 2005. Nanomedicine — foreword. Dm Disease-A-Month 51, 322–324.

Weinstein, B.M., Stemple, D.L., Driever, W., Fishman, M.C., 1995. Gridlock, a localized heritable vascular patterning defect in the zebrafish. Nat. Med. 1, 1143–1147.

Westerfield, M., 1995. The Zebrafish Book. A Guide for the Laboratory Use of Zebrafish (Danio rerio), 3rd Edition. University of Oregon Press, Oregon.

Wittbrodt, J., Shima, A., Schartl, M., 2002. Medaka—a model organism from the Far East. Nat. Rev. Genet. 3, 53–64.

Wu, W., Wieckowski, S., Pastorin, G., Benincasa, M., Klumpp, C., Briand, J.P., Gennaro, R., Prato, M., Bianco, A., 2005. Targeted delivery of amphotericin B to cells by using functionalized carbon nanotubes. Angew. Chem. Int. Ed. Engl. 44, 6358–6362.

Yamago, S., Tokuyama, H., Nakamura, E., Kikuchi, K., Kananishi, S., Sueki, K., Nakahara, H., Enomoto, S., Ambe, F., 1995. In vivo biological behavior of a water-miscible fullerene: 14C labeling, absorption, distribution, excretion and acute toxicity. Chem. Biol. 2, 385–389.

Yang, L., Kemadjou, J.R., Zinsmeister, C., Bauer, M., Legradi, J., Muller, F., Pankratz, M., Jakel, J., Strahle, U., 2007. Transcriptional profiling reveals barcode-like toxicogenomic responses in the zebrafish embryo. Genome Biol. 8, R227.

Yoon, C., Kawakami, K., Hopkins, N., 1997. Zebrafish vasa homologue RNA is localized to the cleavage planes of 2- and 4-cell-stage embryos and is expressed in the primordial germ cells. Development 124, 3157–3165.

Yoong, S., O'Connell, B., Soanes, A., Crowhurst, M.O., Lieschke, G.J., Ward, A.C., 2007. Characterization of the zebrafish matrix *metalloproteinase 9* gene and its developmental expression pattern. Gene Expr. Patterns 7, 39–46.

Zanello, L.P., Zhao, B., Hu, H., Haddon, R.C., 2006. Bone cell proliferation on carbon nanotubes. Nano Lett. 6, 562–567.